Effect of Non-Condensables on Natural Circulation Passive Safety Systems

J.L. Muñoz-Cobo[a], J.C. de la Rosa[a], S. Chiva[a], A. Escrivá[a], L.E. Herranz[b]

[a] Universidad Politécnica de Valencia, Spain.

[b] Ciemat, Spain.

Abstract. The new passive safety systems incorporates passive containment heat exchangers driven by natural circulation as a method to remove the decay heat from the containment, and to transport it by natural circulation to a large pool located outside the containment building. This paper review and evaluate the main existing mechanisms to extract the heat from the containment. First we study the passive containment cooling condensers (PCC), consisting in a set of vertical tubes where the steam and non-condensable mixture circulates down-flow through the tubes that are submerged in a pool. The different existing condensation models are reviewed and evaluated, and then some insights are deduced from the comparisons that have been performed. Then we study the condensation models on finned tubes in presence of non-condensable gases as a method to remove the decay heat from the containment, the results are compared with the experimental data of the thermal-hydraulic phase of the CONGA project.

1. INTRODUCTION

The new passive safety systems used in new reactor designs, incorporate passive containment heat exchangers (HX), driven by natural circulation as a method to remove the decay heat from the containment and to transport it by natural circulation to a large pool located outside the containment and with capability to act as a heat sink at least during 72 hours. The limits to the heat removal are set by the natural circulation flow and the heat removal capability of these HX.

Several HX designs have been incorporated into the passive safety reactors, the first one are the passive containment cooling condensers denoted as PCCCs. Each condenser is formed by a set of vertical tubes connected to common lower and upper headers or drums, and submerged into a water pool. A tube drains the steam plus non-condensable mixture from the containment and drives it to a distributor that transport the mixture by natural circulation to the upper headers of the PCCCs, as it is displayed in figure 1. The upper header is a large cylindrical deposit with the vertical tubes connected to it. This header distributes the gas mixture among the vertical tubes connected to it. Once the gas enters into the tubes, the steam condenses on the walls of the tubes, and the condensation heat is transferred to the PCCC pool. The condensate is drained by gravity to the lower header, where accumulates at the lower part of the lower drum where it is removed by gravity through the drain line which is directly connected to the reactor vessel. The non-condensed steam plus the non-condensable gases are discharged through the vent line into the wetwell pool [1].

Another kind of condensers similar to the PCCC, are the isolation condensers. The isolation condenser system (ICS), removes the decay heat after any reactor isolation during power operations, and consists of four independent loops, each one containing a heat exchanger formed by headers and vertical tubes that condense the steam in the tube side as in the previous PCCCs, and transfer the heat to the IC pool, producing the heating or boiling in the pool water [1].

In these two previous condensers small amounts of non condensable gases deteriorate the condensers performance increasing the pressure loads inside the containment for the PCCC case or inside the reactor vessel in the IC case [2], [3].

The passive containment cooling system loops (PCCS) are driven by the pressure difference created between the containment drywell and the suppression pool. The operation of the PCCS requires no sensing, control, logic or power actuated devices for operation. However, some kind of anti-vacuum breaker is required when the pressure in the wet-well increases 0.5 bar above the drywell pressure, due to the continuous discharge of non-condensable gases and steam in the wet well pool.

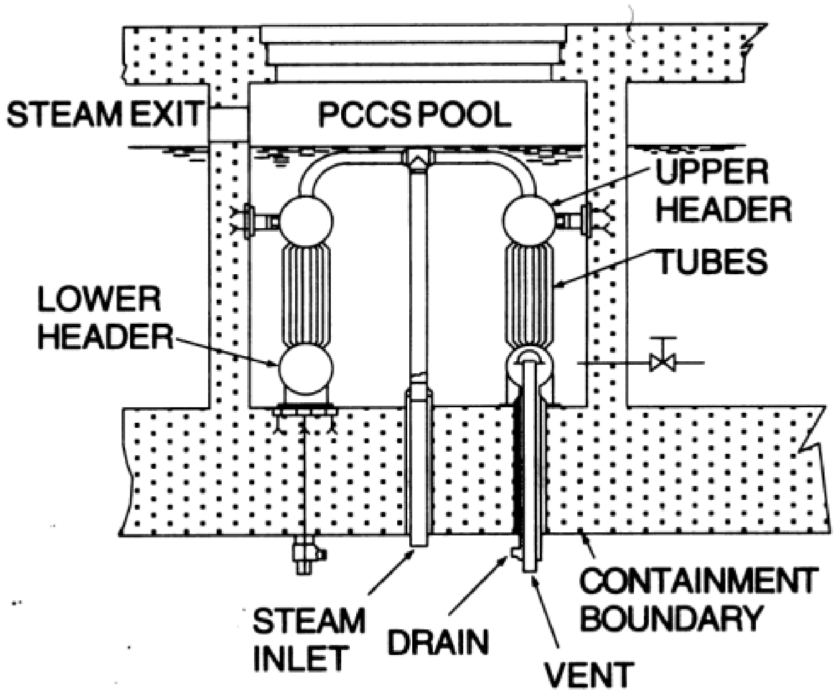

Fig. 1. Passive Containment Cooling Condensers of the ESBWR. The steam plus non-condensables mixture enters through the steam inlet connected to the drywell. In the lower drum the condensed steam is discharged in the reactor through the drain line and the uncondensed steam plus the non-condensable gases are discharged in the wetwell pool through the vent line.

Other reactors like the SWR-1000, use the finned tube containment cooling condensers (FTCCC), these condensers are designed to remove the residual heat from the containment to the dryer separator storage pool located above the containment. These condensers are formed by a set of slightly inclined finned tubes mounted about 1m above the water level of the core flooding pool as displayed at figure 2. These condensers use natural circulation at both sides. At the primary side, if the medium on the heat exchanger after an accident is a nitrogen-steam mixture, then the natural convection flow over the finned tubes is downward toward the core flooding pool, because the density of the nitrogen-steam mixture increases with decreasing temperature. However, the opposite is true for a hydrogen–steam mixture [1], [4], [5].

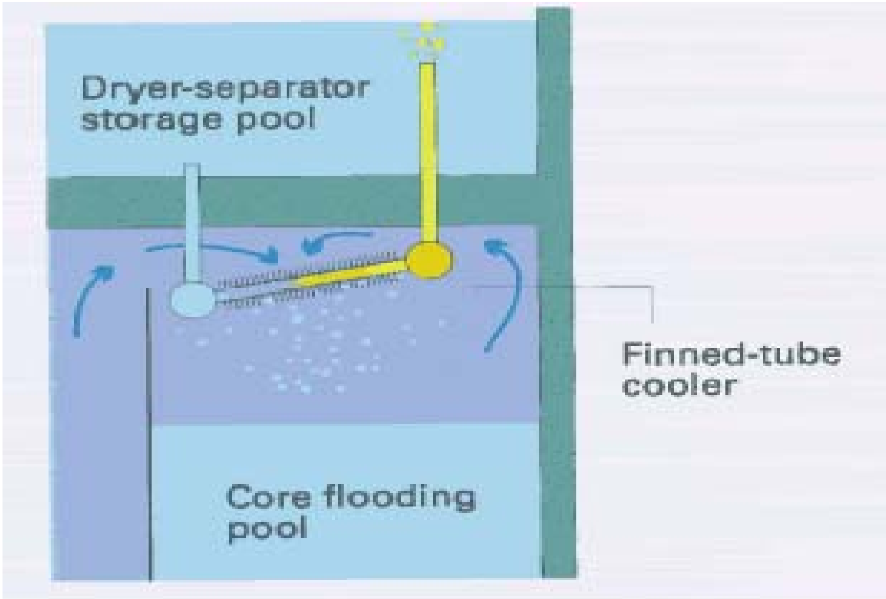

Fig. 2. Finned tube passive containment condenser of the SWR-1000 reactor.

The working principle of FTCCC can be explained as follows: if the temperature in the drywell atmosphere increases over the one in the dryer-separator storage pool, then the steam condenses on the tubes and heat up the water inside the HX finned tubes. This water of less density moves upward by natural circulation due to the slope of the exchangers tubes, and flows through the outlet line, discharging the higher temperature cooling water in the pool. The outlet line ends at a higher elevation level than the inlet line, so the lifting forces are increased for the whole system.

Therefore, in the case of figure 2, we have condensation on the finned tubes in presence of non-condensable gases, but the condensation is on the external surface of the tubes. The opposite happens in the case of figure 1, where the condensation in presence of non-condensable gases takes place inside the tubes and the heat is transfer to the PCC pool.

2. CONDENSATION INSIDE VERTICAL TUBES IN PRESENCE OF NON-CONDENSABLE GASES: DESCRIPTION AND EVALUATION OF CONDENSATION MODELS

The condensation of a mixture of steam and non-condensable gases inside the vertical tubes of the passive containment condensers is a crucial issue for the safety of the passive safety reactors like the ESBWR and the SBWR. The steam and NC gas mixture enters in the upper part of the tubes at high velocity, in this region near the tube entrance the condensation heat transfer dominates over the sensible heat transfer. As condensation proceeds along the tube, the steam partial density diminishes and increases the non-condensable mass partial density. Therefore, the NC mass fraction increases continuously along the tube and becomes very important in the medium and lower part of the tube. As a consequence, the sensible heat transfer becomes more and more important and can dominate over the condensation one especially in the medium and lower region of the tube.

In this section, we describe and evaluate the main condensation models that can be easily implemented in the existing thermal-hydraulic codes, like RELAP, TRAC-BF, and TRACE.

We discuss three models. The first one is the University of California at Berkeley model, denoted as UCB model. This model was developed by Vierow and Schrock, and has been widely used [6]. The advantage of this model is that does not require to iterate or to solve any transcendental equation to find the heat transfer coefficient. Then Kuhn et al. [7] of UCB, developed an improved model denoted UCBA that accounts for interfacial shear effects, but some kind of transcendental equation must be solved. The second model that is analyzed is the UPV-FIT model. This model was developed for the TEPPS project of the EC [3], [8], and gives a good performance in many situations, some equations of the UPV-FIT model have been used for the development of non-iterative condensation models by the Thermal-Hydraulic Research Group of Korea Atomic Research Institute [9]. Finally, the third well known model to be described and evaluated is the METU-TAEA correlation modified by the Sherwood number developed at the METU-CTF test facility, of the Middle East Technical University at Ankara [2], by people of the Turkish Atomic Energy Agency (TAEA).

2.1. Brief description of the University of California Condensation model in presence of NC gases (UCB model)

The simpler UCB model [6] is based on Nusselt theory heat transfer coefficient for condensation without shear and NC effects, multiplied by a degradation factor f(z), where z is the distance measured from the entrance of the tube. This degradation factor is defined as:

$$f(z) = \frac{h_{exp}(z)}{h_{th}(z)} = \frac{h_{exp}(z)\,\delta_N(z)}{k_l} \tag{1}$$

where $h_{exp}(z)$ is the experimental local heat transfer coefficient, and the theoretical one is calculated as $h_{th} = k_l / \delta_N(z)$, where the theoretical local film thickness $\delta_N(z)$ is calculated using Nusselt condensation theory. Finally, in equation (1), k_l is the condensate conductivity. We note that the degradation factor f(z), is a Nusselt number based on the calculated film thickness.

The film thickness $\delta_N(z)$ in this model was derived using Nusselt theory. The mass flow rate per unit of circumferential length denoted by $\Gamma(z)$, can be obtained integrating the liquid mass flux along the film thickness:

$$\Gamma = \frac{W}{\pi d} = \int_0^{\delta_N} dy\, \rho_l\, u_l(z,y) \tag{2}$$

where W is the mass flow rate of the condensate film, d is the inner diameter of the tube and $u_l(z,y)$ is the velocity of the film liquid, y is the radial coordinate measured from the inner surface of the tube. From elementary Nusselt Theory, assuming the film layer as laminar and neglecting interfacial friction forces it is obtained that this velocity is given by:

$$u_l(z,y) = \frac{(\rho_l - \rho_g)g}{\mu}\left(\delta_N(z)y - \frac{y^2}{2}\right) \tag{3}$$

Substituting equation (3), in equation (2), and integrating yields the relation between Γ, and δ_N. That can be reversed to yield:

$$\delta_N(z) = \left[\frac{3\mu_l\,\Gamma}{g\,\rho_l(\rho_l - \rho_g)}\right]^{1/3} = \left[\frac{3\mu_l^2\,Re}{4g\,\rho_l(\rho_l - \rho_g)}\right]^{1/3} \tag{4}$$

Where we have defined the following condensate Reynolds number:

$$Re = \frac{4\Gamma}{\mu} \tag{5}$$

Therefore, the local heat transfer $h_N(z)$ coefficient in the laminar region of the condensate is given by:

$$h_N(z) = \frac{k_l}{\delta_N(z)} = \frac{k_l}{\left[\dfrac{\mu^2}{g\,\rho_l^2}\right]^{1/3} Re_l^{1/3} \left[\dfrac{3}{4}\right]^{1/3}} \tag{6}$$

Therefore, we can define the following Nusselt number in the laminar region

$$Nu = \frac{h_N\, l_e}{k_l} = 1.1\, Re_l^{-1/3} \tag{7}$$

where the characteristic length l_e is defined as $l_e = \left[\nu_l^2 / g\right]^{1/3}$, with ν_l being the kinematics viscosity. Proceeding in a similar way in the turbulent region one finds the following expression for the Nusselt number:

$$Nu = \frac{h_N\, l_e}{k_l} = 0.0195\, Re_l^{1/3} \tag{8}$$

The heat transfer coefficients obtained from equation (7) and (8), must be multiplied by the degradation factor f_{UCB}, this degradation factor was obtained by Vierow and Schrock and then improved by Kuhn et al. The expression of Vierow and Schrock is expressed as [6]:

$$f_{UCB} = f_1\ f_2 \tag{9}$$

The f_1 factor is always greater than one and takes on account the augmentation in the heat transfer coefficient produced by the interfacial shear stress of the gas mixture, that makes thinner the condensate layer.

Vierow and Schrock have correlated this augmentation factor in terms of the Reynolds number of the mixture:

$$f_1 = 1 + 2.88 \times 10^{-5}\ Re_g^{1.18} \tag{10}$$

The degradation factor f_2, was correlated based on experiments with non-condensable gases. For air, this factor is given by the following expression [6]:

$$f_2 = 1 - C\, M_{nc}^{b} \tag{11}$$

where the constants C and b take the following values:

$$\begin{aligned} &C = 10 \quad ; \quad b = 1 \quad M_{nc} < 0.063 \\ &C = 0.938\,;\, b = 0.13 \quad 0.063 < M_{nc} < 0.6 \\ &C = 1 \qquad ; b = 0.22 \quad M_{nc} > 0.6 \end{aligned} \tag{12}$$

This model was improved by the Knuhn-Schrock-Peterson correlation denoted as UCBA, that takes on account the waviness of the condensate layer and the interfacial shear stress, but the model is more complex because involves to solve the Nusselt liquid film boundary layer equation with specified shear stress at the interface and is not as direct ,as the Vierow Schrock model, because it is necessary to iterate to solve this equation.

The degradation factor of the University of California advanced correlation UCBA [2], [7] can be written as follows:

$$f_{UCBA} = f_l\ f_2 \tag{13}$$

where the enhancement factor f_l, is given by:

$$f_l = \left(1.0 + C_{1,UCBA}\ Re_l\right)\frac{\delta_1}{\delta_2} \tag{14}$$

where Re_l is the Reynolds number of the condensate, δ_1 is the film thickness without interfacial shear effects, and δ_2 is the film thickness including shear stress effects. Finally $C_{1,UCBA}$ is a model constant.

The degradation due to air is taken on account by means of an expression of the form:

$$\begin{aligned} f_2 &= 1..0 - C_{2,UCBA}\ M_{nc}^{a} \quad \text{for} \quad M_{nc} < 0.1 \\ f_2 &= 1.0 - M_{nc}^{b} \quad \text{for} \quad M_{nc} > 0.1 \end{aligned} \tag{15}$$

where $C_{2,UCBA}$, a and b are model constants and M_{nc} is the mass fraction of NC gases.

2.2. Brief Description of the METU-TAEA Correlation Model Modified by the Sherwood Number

In this case the degradation factor f is given by:

$$f_{MET} = f_l\ \ f_2 \tag{16}$$

Where f_{MET} is the degradation factor of the Nusselt theory; f_l is the enhancement factor produced by the thinning of the film layer due to the shear stress of the high velocity gas mixture acting on the liquid-gas interface. Also this enhancement factor takes into account the enhancement in the heat transfer produced by the onset of disturbance waves at the interface at relatively low condensate Reynolds numbers. f_2 is the suppression factor.

The enhancement factor f_l is written in the METFU-TAEA model as follows:

$$f_l = f_{SHEAR}\ f_{OTHER} \tag{17}$$

with

$$f_{SHEAR} = \frac{\delta_1}{\delta_2} \tag{18}$$

where δ_1 is the film thickness without interfacial shear stress, and δ_2 is the film thickness with interfacial shear stress. We note that the interfacial shear stress is influenced by both the interface velocity and the mixture side velocity. The entrainment from a liquid film is associated with the onset of disturbance waves at the interface and in general depends on both the gas flow rate and the condensate flow rate. For this reason f_{OTHER} in equation (17), is correlated as:

$$f_{OTHER} = 1 + C_1\ Re_l^{Z_1} + C_2\ Re_g^{Z_2} \tag{19}$$

Where C_1, C_2, Z_1, and Z_2, are constants of the model, Re_l and Re_g are the Reynolds numbers of the condensate and the gas plus NC mixture respectively.

The NC gases move convectively toward the liquid gas interface with the steam and accumulate at the interface producing a degradation in the heat transfer. The accumulation of NC gases at the interface produces a gradient in the radial direction between the interface and the bulk that causes by the Fick law a diffusion of NC away from the interface. Therefore, one needs a non-dimensional number that characterizes the degradation in the heat transfer produced by the NC gases, according to Aglar and Tanrikut [2], this goal can be achieved with the help of the Sherwood number. Therefore, the suppression factor is written as:

$$f_2 = 1 - C_3 \left[y_{nc}\ Sh \right]^{Z_3} \tag{20}$$

where C_3, and Z_3 are model constants, y_{nc} is the NC molar fraction and Sh is the Sherwood number.

2.3. Brief Description of the UPV-FIT model

The local heat transfer coefficient h is expressed as the product of the local heat transfer coefficient k_l/δ, without NC effects, by a degradation factor f due to NC, and other effects. This factor accounts for the degradation in the heat transfer due to the presence of NC gases in the gas mixture and also for the model defects to predict correctly the condensate layer thickness δ. In this way, the heat transfer coefficient is expressed as:

$$h = \frac{k_l}{\delta} f \tag{21}$$

Obviously, we need to compute the condensate film thickness δ and the degradation factor f.

The standard condensation models [3] to calculate δ relate the condensate layer thickness with the distance z to the point where condensation begins. Instead of this, we need in the computational codes like TRAC-BF1 to relate δ with the condensate Reynolds number Re_l. To find this relation we proceed as follows:

The expressions for the local Nusselt number for condensation over a flat plate, on account of the waviness of the condensate layer, are given in the laminar regime according to Mills [10]:

$$\begin{aligned} Nu &= 1.1\ Re_l^{-1/3} \quad \text{for} \quad Re_l < 30 \\ Nu &= 0.822\ Re_l^{-0.22} \quad \text{for} \quad Re_l > 30 \end{aligned} \tag{22}$$

where Re_l is the Reynolds number of the condensate layer, and Nu is the local Nusselt number. The first expression assumes laminar regime while the second one is for laminar-wavy regime.

The local Nusselt number in expressions (22) is given by:

$$Nu = \frac{h\ l_e}{k_l} \quad (1)$$

where h is the heat transfer coefficient, k_l is the condensate conductivity, and l_e is an equivalent length defined by:

$$l_e = \left[\frac{\mu_l^2}{\rho_l^2\ g} \right]^{1/3} \tag{24}$$

where μ_l is the dynamic viscosity and ρ_l the condensate density. From expressions (22) it is obtained that the condensate layer thickness for condensation over a plane plate is given by:

$$\delta_N = 0.909\ Re_f^{1/3}\ l_e \quad \text{for } Re_l < 30 \tag{25}$$

$$\delta_N = 1.2165\ Re_f^{0.22}\ l_e \quad \text{for} \quad Re_l > 30 \tag{26}$$

where the subindex N means that this thickness is obtained from Nusselt theory, with the laminar wavy correction for $Re_l > 30$.

Recently, Cheon and Sik of Korea Atomic Research Institute [9], have developed a non iterative model for steam condensation in the presence of a NC gas inside vertical tubes. They have checked the ability of Muñoz-Cobo et al. expression to predict accurately the film thickness inside a vertical tube without any kind of iteration when interfacial shear forces are considered.

The idea is to substitute in Muñoz-Cobo et al. expression for the condensate layer thickness δ inside a vertical pipe [3], the Nusselt thickness δ_N given by equation (25), or (26), depending on the condensate Reynolds number. In this way, one obtains the following expression for the condensate layer thickness in the laminar or laminar wavy regime in terms of the condensate Reynolds number:

$$\delta = \frac{1.259\ \delta_N^{4/3}}{\left[\delta_p \sum_{j=1}^{2} a_j\, x_p^{j-1} + l_i \sum_{j=1}^{3} b_j\, x_p^{j-1} + m_i\, \delta_p \left(c_1 + c_2\, x_p \right) \right]^{1/3}} \tag{27}$$

Where the value of the constants a_j, b_j, c_j are given by:

$$\begin{aligned} &a_1 = 2\,;\ a_2 = -\frac{28}{15}\,;\ a_3 = -\frac{1}{3} \\ &b_1 = \frac{4}{3}\,;\ b_2 = -2\,;\ b_3 = \frac{8}{15}\,;\ b_4 = \frac{1}{3} \\ &c_1 = \frac{1}{2}\,;\ c_2 = -\frac{8}{15} \end{aligned} \tag{28}$$

and we have defined δ_p as the condensate film thickness inside a vertical pipe, neglecting interfacial shear forces. This thickness is given by the expression [3]:

$$\delta_p = \frac{1.189\ \delta_N}{\left(1 + a_1'\, x_N + a_2'\, x_N^2\right)^{1/4}} \tag{29}$$

x_p is the ratio of δ_p, and the inner tube radius R:

$$x_p = \frac{\delta_p}{R} \tag{30}$$

where x_N in equation (29), is the ratio of the condensate thickness computed with expressions (25) or (26), and the tube radius:

$$x_N = \frac{\delta_N}{R} \tag{31}$$

and

$$a_1' = -\frac{4}{5}\,;\ a_2' = -\frac{1}{3} \tag{32}$$

Finally, the coefficients l_i and m_i depend on the interfacial shear stress, and the friction factor of the steam/Non Condensable (NC) mixture respectively, and are given by:

$$l_i = \frac{2\ \tau_{if}}{\left(\rho_f - \rho_g^* \right)\ g} \tag{33}$$

and

$$m_i = \frac{180\ f_g\ \rho_g\ \left(u_g - u_i \right)^2}{\left(\rho_l - \rho_g^* \right)\ g\ R} \tag{34}$$

where τ_{if} is the interfacial shear stress acting on the condensate layer, f_g is the friction factor of the steam/NC mixture, ρ_g^* is the fictitious density of the steam/NC mixture [3], and u_g is the steam/NC mixture velocity respectively, ρ_g is the mixture density. Finally, u_i is the condensate layer velocity at the interface. Then, the heat transfer coefficient without NC effects is given by k_f/δ.

To estimate the degradation factor f, which appears in expression (21), we use a function based on the observed dependence of h_{exp}/h_{model}, with the mixture Reynolds number Re_g, and the non-condensable mass fraction MNC. The degradation factor can be expressed in the form:

$$f = f_1(Re_g)\ f_2(M_{NC}) \tag{35}$$

$$f_2 = 1 - P_1\ M_{NC}^{P_2} + P_3\ e^{-(P_4\ M_{NC})} \tag{36}$$

where Re_g is the mixture Reynolds number of the steam & NC gas mixture, MNC is the non-condensable mass fraction, and P_1 to P_4 are parameters to be obtained by a non linear regression procedure. This method will be denoted by UPV-FIT model throughout the paper. We have decided to take f_1, equal to one in this model because the model itself contains the thinning effect of the film layer due to the shear stress produced by the gas mixture. Also, the model contains the wavy effects of the condensate layer so we do not need to introduce any additional correlation in f_1, that in general depends on the experimental conditions, and produces big errors when the conditions to be simulated are not similar to the experimental ones.

The parameter values were obtained by a non linear regression procedure using the MINUIT code [11]. To this end, we defined the model degradation factor values to be fitted as:

$$f_i = \frac{h_{exp,i}}{h_{model,i}} \tag{37}$$

where $h_{exp,i}$ denotes the experimental heat transfer coefficient for the i-th case, and $h_{model,i}$ the results of the model when NC gases effects are neglected. The experimental data used were the runs of Vierow and Schrock, without temperature inversion [6].

The parameter values obtained by means of the non linear regression algorithms of the MINUIT code were:

$$P_1 = 1.0266\ ;\ P_2 = 0.12791\ ;\ P_3 = 0.78074\ ;\ P_4 = 29.122 \tag{38}$$

We must point out here that the UPV-FIT model with the parameter values (38) can be applied to a broad range of conditions, because we have fitted only the dependence with the mass fraction of NC.

2.4. *Evaluation of Condensation Models inside Tubes in Presence of NC Gases*

In this section, we perform an evaluation of the different models for steam condensation inside vertical tubes in presence of NC gases. The models that will be evaluated are: i) the UCB model developed by

Vierow and Schrock, the UCBA model developed by Kuhn, Schrock and Peterson, the METU-TAEA model developed by Tanrikut and Aglar, and finally, the UPV-fit model developed by Muñoz-Cobo and Chiva.

First, we compare the results of the UCBA and METU-TAEA models. This comparison was performed by Aglar and Tanrikut [2]. They used the University of Berkeley data base [12] to perform the comparison and defined an average of the absolute values of the relative differences in % between the calculated h_{cal} and experimental h_{exp} heat transfer coefficients as:

$$\varepsilon_r(\%) = \frac{1}{n}\sum_{i=1}^{n}\left|\frac{(h_{cal,i} - h_{exp,i})}{h_{exp,i}}\right|100 \tag{39}$$

The results of this comparison are displayed at table 1.

The results displayed at table 1 show that the correlation found by Aglar and Tanrikut is apparently better than the Kuhn et al correlation (UCBA).

In order to evaluate the UPV fit model we have computed the relative error defined by equation (39), for the Vierow-Schrock model (UCB) model and for the UPV fit model, for the cases of Vierow runs without temperature inversion. The relative errors in % obtained for the different runs are displayed at table 2.

Also we evaluated a mixed model defined as

$$h_{model} = \frac{k}{\delta_{UPV}} f_{2,UCBA}(M_{NC}) \tag{40}$$

where δ_{UPV} is the condensate film thickness calculated with expression (27), and $f_{2,UCBA}(M_{NC})$ is the Kuhn et al. degradation factor for non-condensable gases, in spite that the correlation for non-condensable gases was fitted to another set of experiments however the relative error is 35.56, close to the UCB model results.

Table 1. Comparison of UCBA and METU-TAEA correlations

<table>
<tr><td rowspan="2">Pure Steam</td><td colspan="3">Values of $\varepsilon_r(\%)$ defined by equation (39)</td></tr>
<tr><td colspan="2">$f_{exp}>1.4$</td><td>$f_{exp}<1.4$</td></tr>
<tr><td>METU-TAEA</td><td colspan="2">5.26</td><td>7.18</td></tr>
<tr><td>UCBA</td><td colspan="3">10.57</td></tr>
<tr><td colspan="4"></td></tr>
<tr><td rowspan="2">Steam plus NC gas correlations are based on M_{nc}</td><td colspan="3">Values of $\varepsilon_r(\%)$ defined by equation (39)</td></tr>
<tr><td colspan="2">$M_{nc}<0.1$</td><td>$M_{nc}>0.1$</td></tr>
<tr><td>METU-TAEA</td><td colspan="2">10.23</td><td>18.39</td></tr>
<tr><td>UCBA</td><td colspan="2">12.41</td><td>20.58</td></tr>
<tr><td colspan="4"></td></tr>
<tr><td rowspan="2">Mixture of Steam plus NC. The correlations are based on Sh.</td><td colspan="3">Values of $\varepsilon_r(\%)$ defined by equation (39)</td></tr>
<tr><td>y_{nc} Sh <5</td><td>5<y_{nc} Sh< 25</td><td>y_{nc} Sh > 25</td></tr>
<tr><td>METU-TAEA</td><td>17.22</td><td>16.17</td><td>9.16</td></tr>
</table>

Table 2. Relative errors in % of the condensation models with NC for Vierow and Schrock experiments.

	Relative error $\varepsilon_r(\%)$, defined by equation (39)				M_{nc}
Model	UCB model	UPV-4P	UPV-VS model	UPV-2P	
Run 4	3.8	23.1	22.3	21.7	0.0086
Run 5	14.6	14.9	12.2	19.1	0.023
Run 6	30.2	38.2	24.9	39.0	0.110
Run 7	14.1	13.7	9.1	23.7	0.025
Run 8	18.3	18.5	9.3	31.6	0.024
Run 11	37.4	18.2	41.2	14.8	0.110
Run 12	17.6	20.7	15.7	19.0	0.091
Run 13	18.4	21.4	15.6	23.4	0.13
Run 19	147.2	27.9	181.6	21.6	0.11
Run 21	11.9	17.4	5.7	17.6	0.061
Run 22	35.1	39.7	30.7	46.6	0.037
Run 23	26.3	18.9	10.3	19.7	0.051
Run 24	25.7	35.6	26.7	40.2	0.051
Run 26	48 .3	57.1	79.9	47.7	0.08
Run 28	32.3	18.7	17.2	25.0	0.039
	Average Relative Error of all the Runs $\bar{\varepsilon}_r(\%)$				
	32.1	25.6	33.4	27.3	

Finally, we perform a very simple model with only two parameters, denoted as UPV-2P. In this model, the heat transfer coefficient is calculated as:

$$h_{UPV-2P} = \frac{k_f}{\delta_{UPV}} f_{2,UPV2P}(M_{nc}) \tag{41}$$

with the degradation factor due to non-condensables given by:

$$f_{2,UPV2P} = 1. - 1.0275\, M_{nc}^{0.12807} \tag{42}$$

This model gives an average relative error of 27.3, for all the runs displayed at table 2.

3. STEAM CONDENSATION ON FINNED TUBES HEAT EXCHANGERS IN PRESENCE OF NON-CONDENSABLE GASES

If a severe accident occurs in a nuclear power plant, then large amounts of steam and aerosols will enter to the containment, increasing the pressure and the temperature inside the containment building. To reduce these thermal and pressure loads, the next generation of European Passive Nuclear Power Plants (SWR 1000), incorporates into the containment passive heat exchangers (HX) driven by natural circulation. These passive HX condense the steam inside the containment and transport by natural circulation the heat to a large pool with capability to act as a heat sink at least during 72 hours.

These innovative passive systems consist of several units of horizontal or slightly inclined finned tubes bundles internally cooled by water. The cooling water is heated inside the tubes by the condensation and convective heat removed from the containment, and it is moves by natural circulation to a large pool located outside the containment.

The main problem that arises in this kind of HX is the degradation in the heat transfer produced by the non-condensable gases and the aerosols that are present in large amounts after a severe accident inside the containment. This degradation can increase the containment loads after a severe accident and we must be able to predict this effect as better as possible. In this section, we explain the condensation model onto finned tubes HX in presence of non-condensable gases.

The two main condensation models onto finned tube HX are the Adamek and Murata models [13], [14], the first one is more precise but more complex because it requires a complex iteration procedure to compute the fin's efficiency. The second one is simpler and gives a direct expression to compute the fin's efficiency. Both models according to Muñoz-Cobo et al. [15], can be combined into a single one that is faster and precise.

The total thermal resistance from the bulk gas to the coolant is formulated as a parallel combination of the convective and condensation gas resistances coupled in series to those of condensate layer, the wall, and the coolant. The condensate layer thermal resistance is calculated by means of an Adamek-based condensation model [13]. The gas mixture (Steam plus NC) thermal resistance is formulated based on a diffusion layer modeling [16]. The model results are compared with available experimental data of the thermal-hydraulic phase (steam+non-condensable gases), of the experiments of the CONGA project of the European Community [17].

3.1. Heat transfer global approach

The overall heat flux from the containment bulk gas mixture at temperature T_b, to the coolant circulating inside the finned tube at temperature T_c, is given by Newton's law of cooling:

$$q'' = h_T (T_b - T_c) \tag{43}$$

where h_T is the global heat transfer coefficient which is defined with respect to the outer plain surface area A_0, and is given by the following expression [5]:

$$h_T = \frac{1}{A_0}\left(\frac{1}{R_{cool} + R_{wall} + R_{cl} + R_{gas}}\right) \tag{44}$$

where R_{cool} denotes the coolant thermal resistance, R_{wall} denotes the tube wall thermal resistance, R_{cl} is the condensate layer thermal resistance and, finally, R_{gas} is the gas diffusion layer thermal resistance. Figure 3 displays the set of thermal resistances and temperatures that are encountered from the bulk gas mixture to the coolant circulating inside the finned tube.

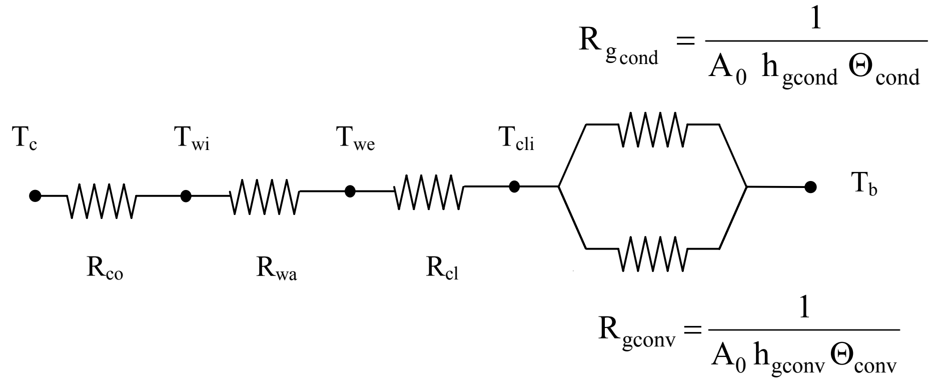

Fig. 3. This figure displays the thermal resistances and temperatures encountered from the bulk gas at temperature T_b, to the coolant at temperature T_c. Also, this figure displays the parallel combination of the condensation and convection gas thermal resistances. T_{wi} and T_{we} are the temperatures at the internal wall and the external wall (fin's root) respectively, and T_{cli} is the temperature at the gas-liquid interface.

The thermal resistance of the gas diffusion layer R_{gas} is calculated as a parallel combination of the convection and condensation gas thermal resistances denoted by R_{gconv} and R_{gcond}, respectively.

3.2. Thermal resistance of the gas diffusion layer

The heat transfer from the bulk gas mixture to the gas-liquid interface has two contributions, one is the condensation heat due to the latent enthalpy released by the steam condensing when reaching the interface, and the other one is the sensible heat transferred through the diffusion layer to the interface [5]:

$$\begin{aligned} q''_{gi} &= q''_{g,conv} + q''_{g,cond} = (h_{g,conv}\,\Theta_{conv} + h_{g,cond}\,\Theta_{cond})(T_b - T_{cli}) \\ &= \left[\frac{Nu\, k_g}{d}\Theta_{conv} + \frac{Sh\, k_{cond}}{d}\Theta_{cond}\right](T_b - T_{cli}) \end{aligned} \tag{45}$$

where $h_{g,cond}$ is the condensation heat transfer coefficient (HTC) of the gas boundary layer, Θ_{cond} is the suction factor for condensation, $h_{g,conv}$ is the convection heat transfer coefficient of the gas, and finally, Θ_{conv} is the suction factor for convection. These suction factors are caused by the boundary-layer shrinkage produced by the transfer of momentum from the gas mixture to the condensate film.

The condensation HTC is related to the Sherwood number Sh, suitable for mass transfer processes, while the convection HTC is related to the Nusselt number. d is the characteristic diameter over which condensation takes place, and k_{cond} is the condensation conductivity given by Peterson expression [16].

$$k_{cond} = \frac{D\, h_{pfg}^2\, C_g\, M_{st}}{R\, T_{avg}^2} \frac{X_{st,avg}}{X_{nc,avg}} \tag{46}$$

where D denotes the air-steam diffusion coefficient, h_{pfg} is the specific enthalpy of phase change plus the subcooling energy to the average condensate temperature, C_g is the gas mixture molar concentration, M_{st} is the molecular weight of the steam, R is the universal gas constant, T_{cli} is the temperature at the gas-liquid interface, finally $X_{st,avg}$ and $X_{nc,avg}$ are the molar fraction logarithmic averages of the steam and non-condensable respectively. We note that the condensation conductivity k_{cond} depends on the diffusion layer average temperature T_{avg}, which must be calculated iteratively.

The convection HTC of the gas mixture is related to the Nusselt number ($Nu = h_{gconv} d_f / k_g$), where the Nusselt number depends on the convection regime. Three different correlations have been used to calculate the Nusselt number: the Churchill and Chu correlation for free convection regime [18]; the Churchill and Berstein correlation [19], for forced convection with Peclet number bigger than 0.2; and the Nakai and Okazaki correlation for slow flow with Peclet number smaller than 0.2 [20]. The Sherwood number of equation (45) is obtained from the same correlations quoted earlier and using the heat and mass transfer analogy, which allows Sh to be correlated as the Nu, provided that the Prandtl number of the gas mixture Pr_g, is substituted by the Schmidt number, $Sc_g = \mu_g / (\rho_g D)$. The properties in the previous equations are average properties of the steam and non-condensables mixture. The heat and mass transfer analogy is known to be accurate enough for low mass flux systems, and correction factors, $\Theta_{i's}$, are introduced to account for the enhancement of transport processes ($\Theta_{i's} > 1$), that takes place in high condensing scenarios. This phenomenon, called suction, is due to the boundary layer shrinkage caused in the liquid film by the steam condensing with higher momentum than the condensate. Under condensation conditions, the suction factor is given by [21]:

$$\Theta_{cond} = \frac{\ln\left(\dfrac{1 - X_{st,b}}{1 - X_{st,i}}\right)}{\left(\dfrac{X_{st,i} - X_{st,b}}{1 - X_{st,i}}\right)} \tag{47}$$

where $X_{st,b}$ and $X_{st,i}$ are the steam molar fractions at the bulk and the interface respectively.

Suction effects on the convective term are accounted for by introducing the following factor into equation (45) [5]:

$$\Theta_{conv} = \frac{a_1}{1 - e^{-a_1}} \tag{48}$$

where the exponent a_1 is given by:

$$a_1 = \frac{C_g M_g c_{pg} D}{k_g} \frac{X_{nc,i} - X_{nc,b}}{X_{nc,avg}} \tag{49}$$

where M_g is the average molecular weight of the gas mixture, c_{pg} is the specific heat at constant pressure of the gas mixture, k_g is the conductivity of the gas mixture, and finally, $X_{nc,i}$ and $X_{nc,b}$ are the non-condensable molar fractions at the interface and the bulk respectively.

3.3. Condensate thermal resistance

In modelling the condensation of steam on finned tubes, the first step is to split the finned tube into three condensation zones according to the amount of condensate that we have in the interfin space (See Figure 4). These zones are:

(1) The unflooded zone, where the interfin space is not completely full of condensate and condensation can take place on the fin tips, fin sides, or fin root depending on the level of condensate from the root.
(2) The flooded zone, where the interfin space is completely full of condensate and condensation can take place only on the fin tips.
(3) The drop-off or pendant zone where condensation is not possible because gravity forms a pendant of condensate that insulates the fin tips.

The condensate layer thermal resistance R_{cl} is related to the condensation heat transfer coefficient h_{cl} of the fin by:

$$R_{cl} = \frac{1}{A_0\, h_{cl}} \tag{50}$$

where h_{cl} is estimated by integration of the condensing heat released per unit length along the circumferential length of the finned tube.

The condensation HTC is given according to Adamek by [13]:

$$h_{cl} = \frac{4\, N_f L\, h_{pfg}\, \dot{M}_{1/2}}{A_0\, \Delta T} \tag{51}$$

where $\dot{M}_{1/2}$ denotes the total mass condensation rate per one half fin at one side of the tube (the factor 4 accounts for the condensation rate onto the whole surface of one fin), L is the condensing length of the tube, N_f is the number of fins per unit length, finally, ΔT is the difference of temperatures between the temperature at the liquid-gas interface and the temperature at the surface of the tube. If the steam is overheated, h_{pfg} includes the latent heat, the super-heat of the steam, plus the subcooling energy to the average condensate temperature [13], [15].

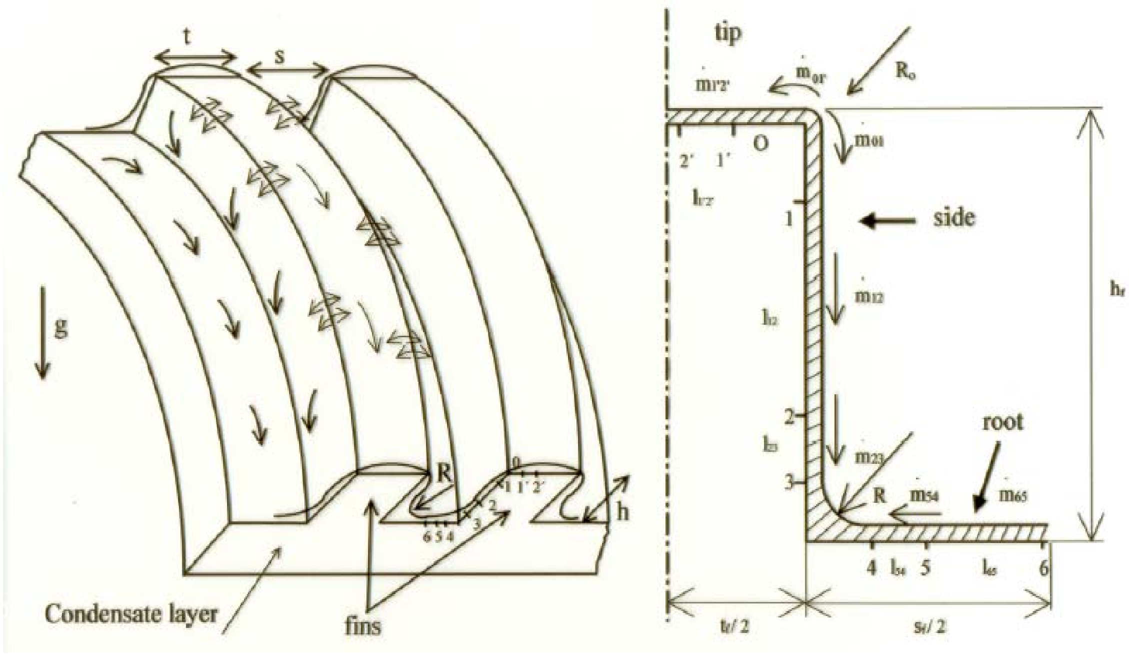

Fig. 4. The left hand side displays the draining flows produced in a finned tube by the steam condensing on the extended surface. The main forces acting on the condensate layer are the gravity and the surface tension. The right hand side displays the transversal section of half a single fin, and the different condensing regions of the fin according to Adamek model [13].

According to figure 4, $\dot{M}_{1/2}$ is computed by means of integration of the mass condensation rates per unit length in the different fin regions along the circumferential coordinate of the fin [15].

Therefore, the total mass condensation rate per one half fin is obviously obtained from the expression:

$$\dot{M}_{1/2} = \dot{M}_f + \dot{M}_u \tag{52}$$

where $\dot{M}_f$ and $\dot{M}_u$ denote the mass condensation rates in the flooded and unflooded regions of one half fin at one side of the tube. The surface splitting displayed at figure 4, allows to compute these mass condensation rates as follows [13], [15]:

$$\begin{aligned}\dot{M}_u = {} & \eta_{fin}\left[\frac{d_f}{2}\int_0^{\psi_0} d\psi\,(\dot{m}_{tip}(\psi) + \dot{m}_{01}(\psi)) + \frac{d_m}{2}\int_0^{\psi_0} d\psi\,\dot{m}_{12}(\psi)\right] \\ & + \eta_{con}\frac{d_m}{2}\int_0^{\psi_0} d\psi\,\dot{m}_{23}(\psi) + \frac{d_r}{2}\int_0^{\psi_0} d\psi\,\dot{m}_{bot}(\psi)\end{aligned} \tag{53}$$

where η_{fin} is the average efficiency in the fin region (tip plus region close to the tip 0-1,1-2), η_{con} is the average efficiency in the connecting region (2-3), ψ_0 is the flooding angle measured from the top of the finned tube, as it is well known this angle defines the frontier of the flooded zone, d_m and d_r are the diameters at the middle of the fin and at the fin root respectively, $\dot{m}_{ij}(\psi)$ is the mass condensing rate in the i-j region per unit of circumferential length, at angle ψ. The efficiencies have been computed by means of Murata model using the equivalency between regions of Adamek and Murata models defined by Muñoz-Cobo et al. [15].

Finally, the following condensation rates per unit length in the circumferential direction have been defined:

$$\dot{m}_{tip} = \dot{m}_{01'} + \dot{m}_{1'2'} \tag{54}$$

and

$$\dot{m}_{bot} = \dot{m}_{54} + \dot{m}_{65} \tag{55}$$

in this model, no condensation is assumed to occur in the 3-4 region.

The total mass condensation rate per one half fin in the flooded zone is given by:

$$\dot{M}_f = \eta_{fin}\frac{d_f}{2}\int_{\psi_0}^{\psi_p} d\psi\ \ \dot{m}_{tip}(\psi) \tag{56}$$

where ψ_p denotes the angle at the beginning of the drop-off or pendant zone. The individual equations to calculate the mass condensation rates $\dot{m}_{ij}$, between points i and j per unit of tube circumference are obtained from elementary energy and momentum balances [13]. The calculation of the efficiencies in the fin and in the connecting region are based on Murata model [14], [15]. The reason to introduce these efficiencies is that the temperature at the fin's tip is not the same than at the fin's root.

The next thermal resistance R_{wall} is the thermal resistance of the tube that can be calculated from the standard expression for a cylindrical shell of internal diameter d_{in} and external diameter d_r, given by:

$$R_{wall} = \frac{\ln\left(\dfrac{d_r}{d_{in}}\right)}{2\pi k_w L} \tag{57}$$

where d_r denotes the external diameter of the tube (diameter at the root of the fin), d_{in} is the internal diameter of the finned tube, finally k_w is the conductivity of the wall material.

The last thermal resistance encountered from the bulk to the coolant is the coolant thermal resistance R_{cool}, that depends on the coolant regime, and is given by:

$$R_{cool} = \frac{1}{A_0\, h_{cool}} = \frac{1}{\pi L k_{cool}\, Nu_{cool}} \qquad (58)$$

where Nu_{cool} denotes the Nusselt number for the heat transfer process from the tube internal wall to the coolant, that depends on the Reynolds and Prandtl numbers of the coolant, k_{cool} is the thermal conductivity of the coolant at the internal wall boundary layer.

For turbulent flow, Re >3000, h_{cool} is given by the Gnieliski correlation, with the entrance effect correction factor to account for non-developed flow [22]. For laminar and transition flow, h_{cool} is given by Churchill and Ozoe correlation [23], which covers both the entrance and fully developed regions.

3.4. Results and discussion

In this section, the results of the experiments performed at JRC by De Santi [24], and at PSI by Suckow [25], are compared with the results of the program FINSTUBOAE that contains the model for fins condensation explained in the previous sections. We have performed a comparison of the results obtained during the thermal-hydraulic phase of the Suckow et al. experiments [25], when we have only steam in presence of NC gases. After this analysis, we have compared our results with the De Santi et al. experiments [24].

The Suckow experiments were performed at a facility called CESANE (Condensation Experiments in Steam Aerosol Noncondensable Environment). The CESANE facility receives aerosol, steam and non-condensable gas flow at specified experimental conditions from the PSI aerosol generation facility DRAGON [17]. The experimental programme consisted of 7 tests at predefined conditions [17]. Each experiment has two stages, at the first stage or thermal-hydraulic phase, all the thermal-hydraulic magnitudes, including the heat flux, were measured before the aerosol injection, at the second stage or aerosol phase, all the thermal-hydraulic magnitudes were measured again, and, in addition, the aerosol mass deposited on the finned tube was also measured. In this analysis, we are interested only in the results obtained during the thermal-hydraulic phase of the experiments.

Thermal-hydraulic comparisons are set in terms of heat flux (q"), and coolant temperature rise along the tube ΔT. Table 3 displays the comparison between FINSTUBOAE results and Suckow experimental data, during the thermal-hydraulic phase when NC are present in amounts ranging from 51% (experiments A4, A5, A7), to 80% (experiments A1, A2, A3, A6). The prediction errors in %, for the heat flux, range from 1.2% for experiment A6, to 13% in experiment A7. So the results can be considered very good. This means that the physical models of the FINSTUBOAE program, for the steam condensation onto finned tubes in presence of NC gases, work properly under the conditions investigated.

Table 3. Comparison of FINSTUBOAE predictions with experiments during the thermal-hydraulic phase of Suckow et al. experiments [25].

	BWR	BWR	BWR	BWR	PWR	PWR	PWR
	A1	A2	A3	A6	A4	A5	A7
q''_{exp}	8.9	8.4	7.5	8.2	2.0	2.19	2.0
$q''_{predicted}$	8.7	7.8	8.1	8.3	2.15	2.25	2.26
Error %	-2.2	-7.1	8.	1.2	7.5	2.7	13
ΔT_{exp}(ºC)	13.8	12.7	11.0	12.1	4.9	5.7	6.2
ΔT_{pred}(ºC)	13.0	11.8	12.4	12.7	6.0	6.3	6.3
Error %	-5.8	-7.1	12.7	4.7	22.4	10.5	1.6

The JRC integral tests with a large scale PWR heat exchanger unit, were performed with a test vessel similar to CESANE facility [17]. It was connected to the JRC's STORM test facility. The main test conditions can be found in [17].

At table 4 we display the comparison between FINSTUBOAE predictions and experimental data for JRC experiments, during the thermal-hydraulic phase of the experiments. The thermal-hydraulic variables selected to perform the comparison were the heat flux q" at the fins tubes, and the temperature rise of the coolant water ΔT.

From Table 4, we conclude that FINSTUBOAE estimates quite consistently the heat fluxes and coolant temperature increases.

Table 4. Comparison of FINSTUBOAE predictions with measured data of the heat flux q”(KW/m^2), the cooling temperature rise ΔT, on the finned tubes in De Santi et al. experiments [17].

	PWR HX1	PWR HX2	PWR HX3	PWR HX4	PWR HX5
$q”_{exp}$	1.2	2.01	2.16	1.99	1.82
$q”_{predicted}$	1.4	1.35	1.71	1.62	1.67
Error %	16.6	-32.5	-21.	-18.5	-8.2
$\Delta T_{experim}$(ºC)		5.51	5.72	5.43	5.13
$\Delta T_{predicted}$(ºC)	2.32	3.65	4.64	4.41	4.52
Error %		-31.	-19.	-18.8	-11.9

4. CONCLUSIONS AND CONCLUDING REMARKS

In this paper, we have studied different condensation models inside tubes in presence of NC gases, these models in general are based on Nusselt theory and incorporate degradation factors to take into account the degradation in the heat transfer produced by the NC gases. Some models incorporate also enhancement factors that are dependent on the condensate Reynolds Number and the mixture gas Reynolds Number. In this way, they take into account the enhancement in the heat transfer produced by the shear stress on the interface that depends on the mixture Reynolds Number. Also, they consider the enhancement in the heat transfer produced by the waves and ripples at the interface by incorporating an enhancement factor that depends on the Reynolds Number of the condensate.

However, the use of these correlations in the big simulation codes like RELAP, TRACE, ATHLET has the disadvantage that the correlations are valid only for the thermal-hydraulic conditions of the experiments in which the correlations are based, and if we use these correlations outside these conditions, we can have big error in the predictions.

Therefore, it is better to rely on simple models with a broad range of conditions of applicability. In this way, we must point out that the fact that a given correlation gives less error that a given model for a set of runs of a particular experiment, does not mean that this correlation is better, only means that is better for that particular set of experiments, perhaps for other set of experiments with different thermal-hydraulic conditions is much worse.

We have devoted the second part of this work to study the condensation of a mixture of steam and non-condensable gases on finned tubes cooled internally by natural circulation as explained in the introduction.

We have based our study in the well known models of Adamek and Webb [13], [14], and Murata [15]. The degradation in the heat transfer produced by the Non-Condensable gases has been performed by means of a diffusion layer modelling where we consider the sensible and the condensation heat transfer. The comparison with the experimental data gives a good agreement.

ACKNOWLEDGEMENTS

The authors of this work are indebted to the financial help of Ministerio de Ciencia y Tecnología, Plan Nacional de Investigación, Project ENE 2004-06978-C02-01.

REFERENCES

[1] INTERNATIONAL ATOMIC ENERGY AGENCY, Status of advanced light water reactor designs, IAEA-TECDOC-1391, Vienna (2004).

[2] AGLAR, F., TANRIKUT A., Activities of passive cooling applications and simulation of innovative nuclear power plant design, IAEA-TECDOC-1281, Vienna (2002) 115-124.

[3] MUÑOZ-COBO, J.L., HERRANZ, L.E., SANCHO, J., TKACHENKO, I., VERDU G., Turbulent vapor condensation with non-condensable gases inside vertical tubes, Int. Journal heat and Mass Transfer **39** 15 (1996) 3249-3270.

[4] MESETH, J., Natural circulation and stratification in the various passive safety systems of the SWR 1000, IAEA-TECDOC-1281, Natural Circulation Data and Methods for advanced water cooled nuclear power plants designs, Vienna (2002).

[5] HERRANZ, L.E., MUÑOZ-COBO, J.L., and PALOMO, M.J., Modeling condensation heat transfer on a horizontal finned tube in the presence of non-condensable gases, Nuclear Engineering and Design **201** (2000) 273-288.

[6] VIEROW, K.M., Behaviour of steam-air systems condensing in cocurrent downflow, Master Thesis, University of California, Berkeley (1990).

[7] KUHN, S.Z., SCHROCK, V.E, PETERSON, P.F., "An investigation of condensation from steam-gas mixtures flowing downward inside a vertical tube". Proceedings of the NURETH 7 Conference (1995) 312-331.

[8] MUÑOZ-COBO, J.L., CHIVA, S., CORBERAN, J.M., ESCRIVÁ, A., Interaction between convection and condensation heat transfer in the passive containment cooling condensers of the ESBWR, Annals of Nuclear Energy **26** (1999) 277-300.

[9] NO, H.C., PARK, H.S., Non-iterative condensation modeling for steam condensation with non-condensable gas in a vertical tube, Int. Journal of Heat and Mass Transfer **45** (2002) 845-854.

[10] MILLS, A.F., Heat Transfer, Edited by Irwin , USA (1994).

[11] JAMES, F., MINUIT: Function minimization and error analysis, CERN Program Library. Write-up D506. Computing and Networks Division (1994).

[12] KUHN, S.Z., SCHROCK, V.E., PETERSON, P.F., Final report of the U.C. Berkeley, Single tube condensation studies", Dept. of Nuclear Engineering, UCB-NE-4201 (1994).

[13] ADAMEK, T. and WEBB, L., Prediction film condensation on horizontal integral finned tubes, Int. J. Heat Mass Transfer **33** 8 (1990) 177.

[14] MURATA, K., ABE, K., and HASHIZUME, K., Condensation heat transfer in a bundle of horizontal integral-fin tubes, Exp. Heat Transfer **5** (1992) 115.

[15] MUÑOZ-COBO, J.L., PALOMO, M.J. and HERRANZ, L.E., Predictive modeling of steam condensation onto finned tubes in the presence of non-condensable gases for passive safety reactor heat exchangers, Nuclear Technology **134** (2001) 23-36.

[16] PETERSON, P.F., SCHROCK, V.E. and KAGEYAMA, K., Diffusion layer theory for turbulent vapor condensation with non-condensable gases, J. Heat Transfer **115** (1992) 998.

[17] FRIESEN, E., MESET, J., GUENTAY, S., SUCKOW, D., LOPEZ J., HERRANZ L., PEYRES V., DE SANTI, G.F., KRASENBRINK, A., VALISI, M. and MAZZOCHI, L., Containment behavior in the event of core melt with gaseous and aerosol releases (CONGA)", FISA99, EU research in reactor safety. EUR19532EN, Luxembourg (2000).

[18] CHURCHILL, S.H., and CHU, H.H.S., Correlating equations for laminar and turbulent free convection from a vertical plate, Int. J. Heat Mass Transfer **18** (1975) 1323.
[19] CHURCHILL, S.H. and BERSTEIN M., A correlation equation for forced convection from gases and liquids to a circular cylinder in cross-flow", Int. J. Heat Mass Transfer (1977).
[20] NAKAI, S. and OKAZAKI, T., Heat transfer from horizontal circular wire at small Reynolds and Grashof number - I pure convection", Int. J. Heat Mass Transfer **18** (1975) 387-396.
[21] BIRD, R.D., STEWARD, W.E. and LIGHFOOT, E.D., Transport Phenomena, Chap. 21, Wiley-Interscience, New York (1960).
[22] GINIELISKI, G.V., New equations for heat and mass transfer in turbulent pipe and channel flow, Int. Chem. Eng **16** 4 (1976) 359-368.
[23] CHURCHILL, S.H. and OZOE, H., Correlation for laminar forced convection with uniform heating in flow over a plate and in developing and fully developed flow in a tube, J. Heat Transfer **95** (1973) 78.
[24] DE SANTI, F., HUMMEL, R. and KRASENBRINK, A., PWR heat exchangers performance in the presence of soluble and non-soluble aerosols, Topical Report, INNO-CONGA(99)-P009 (1999).
[25] SUCKOW, P.D., GUNTAY, S. and DEHBI, A., Summary report of the results of aerosol tests in the CESANE facility, Topical Report INNO-CONGA(99)-P012 (1999).